Human-Robot Collaborative Cable-Suspended Manipulation With Contact Distinction

Giovanni Cortigiani, *Graduate Student Member, IEEE*, Monica Malvezzi, *Member, IEEE*, Domenico Prattichizzo, *Fellow, IEEE*, and Maria Pozzi, *Member, IEEE*

***Abstract*—The collaborative transportation of objects between humans and robots is a fundamental task in physical human-robot interaction. Most of the literature considers the rigid co-grasping of non-deformable items in which both the human and the robot directly hold the transported object with their hands. In this letter, we implement a control strategy for the collaborative manipulation of a cable-suspended platform. The latter is an articulated and partially deformable object that can be used as a base where to place the transported object. In this way, the human and the robot are not rigidly coupled, ensuring a greater flexibility in the partners' motions and a safer interaction. However, the uncertain dynamics of the platform introduces a greater possibility of unintended collisions with external objects, which must be distinguished from contacts arising when a load is placed on or removed from the platform. This letter proposes a contact detection and distinction strategy to address this challenge. The proposed cable-suspended manipulation framework is based only on force sensing at the robot end-effector, and was tested with ten users.**

***Index Terms*—Human-centered robotics, human-robot collaboration, physical human-robot interaction.**

I. Introduction

THE collaborative transportation of objects between humans and robots allows load sharing between the partners as well as the possibility of co-carrying large objects. These applications are particularly useful in industrial and service settings [1], but could have an important impact also in the assistive field, to help people with upper-limb disabilities [2]. Most of the literature on human-robot co-grasping focuses on carrying rigid objects that are either directly grasped by the collaborators, or held through rigidly attached handles. Thus, the human-object-robot coupling is typically rigid [3], [4], [5], [6], [7], [8], [9], [10], [11]. However, there is a growing trend towards tackling the collaborative manipulation of flexible and deformable items [12], [13], [14], including cases in which the load sharing is mediated by flexible elements in contact with the object [15].

The use of cables can increase the versatility of autonomous robotic systems, including cable-driven parallel robots [16], [17] and cable-suspended cooperative aerial manipulators [18], [19], [20], [21]. In the first case, the robot end-effector pose is controlled by means of extendible cables allowing for a greater workspace than other parallel robots, in the second case, multiple UAVs co-transport loads using a cable-suspended platform, without needing on-board grippers.

This letter tackles the novel scenario of controlling cable-suspended loads that are co-transported by a human operator and a robot manipulator. The proposed concept is sketched in Fig. 1. The idea is that the collaborators transport a platform that is suspended through cables that are attached to the robot end-effector and to a handle held by the operator. The platform is rigid and can be used to place objects over it. The cables extend the robot workspace beyond its limits as, for example, with long cables the platform can reach places that are well below the robot base. In addition, the presence of cables allows the human to keep a certain distance from the robot and ensures that there is

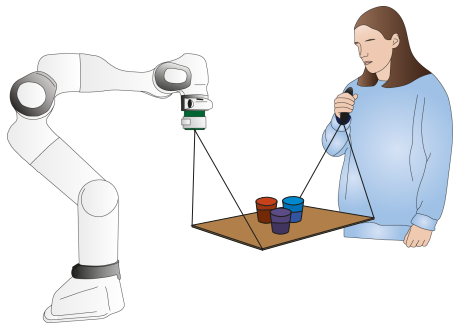

Fig. 1. Collaborative cable-suspended manipulation. The robot follows the human to co-carry cable-suspended loads.

Received 5 July 2024; accepted 20 November 2024. Date of publication 5 December 2024; date of current version 13 December 2024. This article was recommended for publication by Associate Editor Kyle B. Reed and Editor Jee-Hwan Ryu upon evaluation of the reviewers' comments. This work was supported in part by the European Union by the Next Generation EU project ECS17 "THE - Tuscany Health Ecosystem" (PNRR MUR M4 C2 Inv. 1.5, CUP B63C22000680007, Spoke 9: Robotics and Automation for Health) and the Horizon Europe project "HARIA - Human-Robot Sensorimotor Augmentation - Wearable Sensorimotor Interfaces and Supernumerary Robotic Limbs for Humans with Upper-limb Disabilities" Grant 101070292, and in part by the Leonardo S.p.A. under Grant LDO/CTI/P/0025793/22. *(Corresponding author: Giovanni Cortigiani.)*

This work involved human subjects or animals in its research. Approval of all ethical and experimental procedures and protocols was granted by the Ethical Committee of the University of Siena "CAREUS" under Application No. 13/2023.

Giovanni Cortigiani and Monica Malvezzi are with the Department of Information Engineering and Mathematics, University of Siena, 53100 Siena, Italy (e-mail: giovann.cortigiani@student.unisi.it; monica.malvezzi@unisi.it).

Domenico Prattichizzo and Maria Pozzi are with the Department of Information Engineering and Mathematics, University of Siena, 53100 Siena, Italy, and also with the Humanoids & Human Centered Mechatronics Research Line, Istituto Italiano di Tecnologia, 16163 Genoa, Italy.

This letter has supplementary downloadable material available at https://doi.org/10.1109/LRA.2024.3511396, provided by the authors.

Digital Object Identifier 10.1109/LRA.2024.3511396

not a rigid coupling between the collaborators, leading to lower exchanged forces.

To let the robot follow human motions and keep the platform in the desired configuration, in this work an admittance control strategy is proposed. Admittance control is a common choice in physical human-robot interaction (pHRI) [22], and here we adapt it to the envisaged application. The control relies only on force measurements to estimate the direction of the human motion. Thus, there is no need for tracking the human body motions as done, for example, in [15].

To ensure a safe and smooth collaboration, a contact distinction strategy aimed at detecting collisions with external obstacles and at distinguishing them with respect to contacts due to the placement or removal of carried loads is proposed. The contact detection is based on the approach presented in [23], which is adapted to account for the fact that the contacts arise at the platform level and not on the robot body. The contact distinction is implemented with a new threshold-based approach. To the best of our knowledge, previous works on human-robot co-transportation typically do not consider the problem of contact detection and distinction between the co-carried object and external objects.

The proposed methodology has been validated in two different experiments with 10 participants showing the overall usability of the system, as well as its reliability in contact detection and distinction.

II. Related Works

The cooperative manipulation between two or more agents has been widely studied in the field of autonomous multi-robot systems [24], and found new applications in pHRI scenarios where human and robot partners collaboratively carry a load. Usually, the human operator leads the task and the robot has to follow their motion. While there are works that formulate this problem as a trajectory tracking task [10], typically an admittance controller based on force sensing is employed to ensure that the robot(s) follow the human partner while holding a shared load.

Considering recent works on human-robot co-trasportation that adopt admittance control, while some still assume that the manipulated object is rigid [6], [9], [11], as in seminal works like [5], others start considering flexible or deformable items [14], [15], [21].

Solanes et al., [6] propose to combine sliding mode control and admittance control for safe co-transportation, whereas Franceschi et al. [11] tackle this task using distributed Game-Theoretical Model Predictive Control and human intention prediction. In [9], authors propose a method to cope with variable loads during co-transportation. This capability has been integrated in our system too, as, thanks to the collision distinction procedure, it is possible for the user to place/remove loads on/from the platform during the collaboration. However, differently from this letter, Mujica et al. [9] consider that the object is rigid and that the robot has a predefined trajectory to follow.

Regarding the inputs required for controlling the robot, similarly to [6], [9], our method relies solely on force sensing at the robot end-effector, and does not require an external system to track human motions as in other works dealing with deformable objects [14], [15], [21].

In [21], authors propose a novel approach for safe collaborative manipulation of a cable-suspended payload with multiple aerial robots. While the use of inextensible cables is in common with our work, the target robotic system is different. The setup considered in [15] shares some similarities with the one proposed in this letter, as it involves robot manipulators (even though mobile), and the forces transmitted from the human to the robot are mediated by flexible elements. While in [15] flexible straps worn on both human shoulders are used, in this letter we opt for a cable-suspended platform that is held using a single hand. In this way, also potentially dangerous objects can be safely transported and one of the hands is left free to do other tasks.

Despite literature on safety in pHRI has long focused on the detection of collisions between the human and the robot or the robot and its environment [25], as well as on the discrimination between voluntary and unintentional contacts [23], [26], [27], previous works on collaborative transportation usually do not tackle these problems. In pHRI, the classification of contacts is mainly implemented with threshold-based or data-driven methods [27]. The first ones are usually rather fast but require the empirical definition of thresholds and thus might not generalize well to other scenarios [23]. The second ones can better generalize to different settings, but require a training phase and can be rather slow [28]. In this letter, we chose to adopt a threshold-based strategy to ensure a fast robot response to contacts arising between the cable-suspended platform and other objects during the co-manipulation.

III. Methodology

The methodology proposed in this work has two primary objectives. First, the robot must follow the movements of the user to co-carry the cable-suspended platform along the desired trajectory, keeping it in equilibrium and preserving its orientation (Fig. 1). To this aim, an admittance control strategy is proposed. Second, the robot must detect when a contact between the platform and an external object occurs and distinguish the cause of the collision to react properly. Hence a contact detection and distinction algorithm is proposed to let the robot recognize when an object is placed on or removed from the platform, and discriminate these events with respect to a collision with an external obstacle. The system workflow is shown in Fig. 2. After an initial force calibration phase in which the desired force at the end-effector is defined, the collaboration starts. Whenever there is a change in the load placed on the co-manipulated platform, a force calibration is performed again. If a collision with an external obstacle is identified, a safe recovery strategy is triggered. Both the control and the detection strategies only need as input the forces measured at the robot end-effector.

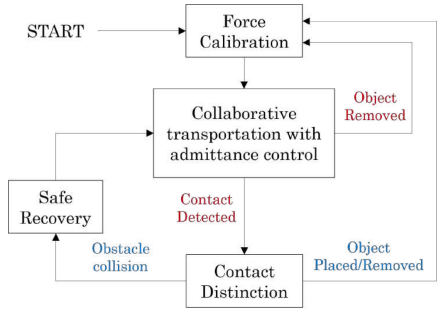

Fig. 2. Workflow of the proposed system. Boxes: task phases. Red text: events that can be detected during the collaboration. Blue text: decisions on the possible contact types.

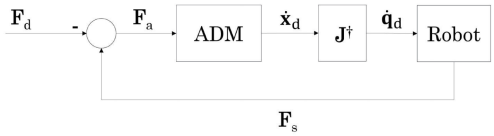

Fig. 3. Block scheme of the proposed control framework. $\mathbf{F}_d$: desired force, $\mathbf{F}_s$: force at the end-effector, $\mathbf{F}_a$: force error, $\dot{\mathbf{x}}_d$: desired end-effector velocity computed according to the admittance law, $\mathbf{J}$: Jacobian of the robot, $\dot{\mathbf{q}}_d$: vector of desired robot joint velocities, ADM: admittance control.

A. Collaborative Transportation With Admittance Control

A common control strategy used to ensure the compliant behaviour of a robot is the Cartesian admittance control, which consists in modelling the dynamics of the robot as a mass-spring-damper system. Following [15], [23], we did not consider the stiffness term in the equation of the dynamics, as the collaboration task is conducted in the free space. The system can then be described according to:

$$\mathbf{F}_a = \mathbf{M}_d\ddot{\mathbf{p}} + \mathbf{D}_d\dot{\mathbf{p}}, \tag{1}$$

where $\dot{\mathbf{p}}$ and $\ddot{\mathbf{p}} \in \mathbb{R}^3$ are the end-effector translational velocity and acceleration, respectively. Since cables are considered as massless, inextensible, and perfectly flexible straight segments, we assume that no torques can be transmitted from the human to the robot, and thus rotational components are not considered in the control equations. These assumptions are reasonable in the scope of this work, where we adopt thin, inextensible cables.

$\mathbf{M}_d$, $\mathbf{D}_d \in \mathbb{R}^{3\times3}$ represent the desired inertia and damping properties of the system, respectively, and are assumed to be diagonal. The choice of inertia and damping parameters entails a trade-off between the accuracy and responsiveness of the system, and needs to be adjusted depending on the envisaged task [29].

Due to the specific features of the proposed system, including the fact that users are not directly in contact with the robot and that the total weight of the cable-suspended load is unknown a priori and may change over time, due to placing/removing different objects on the platform, we do not feed the admittance controller directly with the force measured at the end-effector as in [15], [23], but instead we compute $\mathbf{F}_a \in \mathbb{R}^3$ as detailed in the following and in Fig. 3.

At the beginning of the task, the user positions the platform in a desired configuration and the forces measured at the robot end-effector are averaged over a time t_{set} and stored as the reference signal $\mathbf{F}_d \in \mathbb{R}^3$. This phase is called "Force Calibration", and is repeated whenever an object is placed on, or removed from, the platform, updating the reference signal accordingly (Fig. 2). Then, the input of the admittance controller is computed as $\mathbf{F}_a = \mathbf{F}_s - \mathbf{F}_d$, where $\mathbf{F}_s \in \mathbb{R}^3$ is the filtered version of the raw output of the force sensor placed at the robot end-effector. At each time instant k, the measured force $\mathbf{F}_{raw} \in \mathbb{R}^3$ is filtered using an Exponential Moving Average (EMA) filter such that $\mathbf{F}_s(k) = \alpha\mathbf{F}_{raw}(k) + (1-\alpha)\mathbf{F}_{raw}(k-1)$, where $\alpha \in [0,1]$ is the smoothing factor.

The desired end-effector velocity $\dot{\mathbf{p}}_d \in \mathbb{R}^3$ is obtained according to (1), and the desired joint velocities $\dot{\mathbf{q}}_d \in \mathbb{R}^n$ are computed according to $\dot{\mathbf{q}}_d = \mathbf{J}^\dagger\dot{\mathbf{x}}_d$, where $\dot{\mathbf{x}}_d = [\dot{\mathbf{p}}_d^T\ \mathbf{0}_{1\times3}]^T$, $\mathbf{J} \in \mathbb{R}^{6\times n}$ is the Jacobian matrix of the manipulator, and $(\cdot)^\dagger$ denotes the pseudo-inversion operator. Then, the robot is controlled in velocity to achieve $\dot{\mathbf{q}}_d$.

Note that a certain value of $\mathbf{F}_d$ corresponds to a determined pose of the platform, and thus, trying to achieve that force at the end-effector allows the robot to always keep the platform in the desired configuration, compensating for force variations by moving in the same direction as the human.

B. Contact Distinction

The contact handling strategy proposed in this letter is composed of two main steps (Fig. 2): "Contact Detection", and "Contact Distinction". The former runs in parallel to the co-transportation algorithm and allows to distinguish forces due to the voluntary human interaction from those arising from contacts between the platform and external objects. The latter is executed once a contact is detected and allows to distinguish a collision with an obstacle from a change of the platform payload.

To implement contact detection, we adapt to our scenario the method proposed by Kouris et al. [23] for distinguishing human intended contacts for cooperation from involuntary collisions. Differently from [23], here the contacts arise at the platform level, not directly on the robot structure. The approach is based on the concept that by analysing the forces in the frequency domain, the ones attributed to a collision present a greater magnitude at higher frequencies, whereas collaboration forces present a greater magnitude at lower frequencies [23]. Hence, a collision can be detected by observing the rate of change of the magnitude of the spectrum of the frequency components attributed to a collision. The method is implemented according to the following procedure.

At each time instant, the Fast Fourier transform (FFT) algorithm is applied to a sliding window of N measurements, weighted by a window function w. The magnitude $\mathbf{F}_\omega$ of the discrete Fourier transform of the time series of the jth component of $\mathbf{F}_{raw}$ is (for $\boldsymbol{a} = \mathbf{F}^j_{raw}$):

$$F^j_\omega(m) = \left\| \sum_{n=0}^{N-1} w_n a_n e^{\frac{-2\pi i}{N}mn} \right\|, \quad m = 0, \ldots, N-1,$$

where n and m are the time domain and frequency domain ordinals, respectively. The used window function is a half-Hann

window, defined as:

$$w_n = \frac{1}{2}\left(1 - \cos\left(\frac{2\pi n}{2N-1}\right)\right), \quad n = 0, \ldots, N-1.$$

This type of function gives the maximum importance to current measurements, gradually decreasing the influence of past measurements. The length N of the window is chosen according to the desired frequency resolution $\Delta\omega = \frac{1}{T_s N}$, and by considering that the FFT algorithm performs better with N chosen as a power of 2. The Fourier transform must be analysed in the range of frequencies $[\omega_{\min}, \omega_{\max}]$ corresponding to collisions. Frequencies below $\omega_{\min}$ are attributed to forces due to a voluntary collaboration with the human, whereas frequencies above $\omega_{\max}$ are due to sensor noise. The choice of these boundaries is fundamental to be able to accurately recognize contacts. They depend also on the damping and inertia parameters selected for the admittance control, even though it was demonstrated in [23] that the same frequency boundaries prove to be efficient for a wide range of control parameters. Let us define the Spectral Norm Derivative index as:

$$I^j_{SND} = \frac{d\|\mathbf{F}^j_{\omega_{\min}:\omega_{\max}}\|_1}{dt},$$

where $\mathbf{F}^j_{\omega_{\min}:\omega_{\max}}$ is the frequency components vector in the selected frequency range and $\|\cdot\|_1$ is the 1-norm of the vector which defines the overall magnitude. Hence, I^j_{SND} reflects the rate of change of the jth component of the force in the selected frequency interval, and a contact is detected when the condition $|I^j_{SND}| > I^j_{th}$ is met for at least one of the three components. I^j_{th} is the threshold which defines the distinction and to select it for each component an initial tuning phase is needed (details in Section IV).

The contact distinction procedure starts when a contact is detected. As a first thing, the robot stops and the value $F^z_{s,c}$ is computed. The latter is average of the z component of $\mathbf{F}_s$ computed over a time interval t_c following the collision. Based on the value of $F^z_{s,c}$, different conditions can be distinguished as follows:

$$\begin{cases} F^z_{s,c} - F^z_{\mathrm{d}} > F_{\mathrm{th}} & \rightarrow \text{Object Placed} \\ F^z_{\mathrm{d}} - F^z_{s,c} > F_{\mathrm{th}} & \rightarrow \text{Object Removed} \\ \text{otherwise} & \rightarrow \text{Obstacle Collision} \end{cases} \tag{2}$$

F^z_{d} indicates the z component of $\mathbf{F}_d$, while F_{th} denotes a threshold which determines the minimum change in weight that the algorithm is able to recognize. Hence, the smaller this value, the lighter the object that can be detected by the algorithm. Nevertheless, a too low threshold may prevent the accuracy of the algorithm to detect collisions due to external obstacles. Notice how this approach generalizes over the location in which the object is placed, since, independently from the object location, the recalibration of the force ensures the platform to be held in equilibrium by the robot in the co-transportation. However, the assumption is that no slippage of the object over the platform occurs.

As shown in Fig. 2, in the event of a collision with an obstacle, a policy to recover from it is implemented: the robot moves back to a safe configuration, corresponding to its pose 1 s before the collision, and then resumes the collaboration.

It is worth noting that while placing an object over the platform usually implies a fast impact between the object and the platform, the process of removing an object is typically more gradual. Thus, it might not always be detected as a contact with the previously defined method. To ensure that also smooth object removals are recognized, we implemented an additional routine that runs in parallel with the admittance controller.

Denoting the average of the z component of $\mathbf{F}_d$ over a time t_r with F^z_r, an object removal is detected if: $F_0 - \epsilon < F^z_r < F_0 + \epsilon$, where F_0 is the z component of $\mathbf{F}_d$ computed before the placement of the object on the platform, and ϵ is a parameter describing the tolerance. A high tolerance makes it easier to identify when an object has been removed, but it also increases the risk of misinterpreting the user's movements upwards as a removal of the object (note that both when the user moves upwards and when an object is removed, the z component of the force measured at the robot end-effector decreases). Concerning t_r, it should be sufficiently high to prevent an imprecise measurement of the force, yet it should be sufficiently small to ensure that the removal is identified quickly, avoiding unwanted upward motions of the robot.

IV. Experiments

To evaluate the proposed method, two experiments were implemented, in which users had to pick objects up from an initial position and place them in a final position, using a cable-suspended platform to transport them together with the robot. In both experiments, the user leads the motion of the robot, that follows the operator thanks to the admittance control strategy explained in Section III-A. In Experiment A (Exp. A), users were allowed to move freely, in Experiment B (Exp. B), they had to follow a predefined trajectory. Besides verifying the capability of the robot of following the human during the collaborative task, the two experiments had specific different purposes. The main objective of Exp. A was to show the system capability of distinguishing the placement or removal of objects of different weights and sizes onto or from the platform. Exp. B, instead, aimed at testing the system capability of distinguishing object placement/removal from collisions with external obstacles. In this case, collisions were induced by placing an obstacle along the predefined trajectory.

A. Experimental Setup

The setups for the two experiments are shown in Fig. 4. They both include a collaborative robot arm (Franka Research 3), an ATI gamma F/T sensor (ATI Industrial Automation, Inc., US) attached to the robot end-effector, and a wooden flat platform ($0.50 \times 0.40 \times 0.004$ m, 323 g) connected through inextensible threads to the robot end-effector and to an ergonomic handle held by the user. Additionally, in Exp. A, an OptiTrack motion capture system (NaturalPoint Inc., USA) was used to track the human hand and the platform [30], whereas in Exp. B, the setup included an obstacle (red box) placed along the predefined path and equipped with an ATI nano 17 F/T sensor to detect the exact

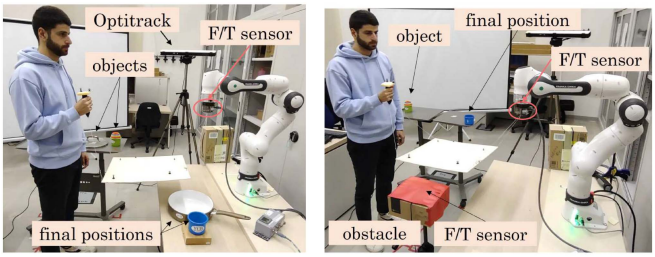

Fig. 4. Experimental setups: Exp. A (left), Exp. B (right).

time instant in which a collision occurred. All the elements were integrated using ROS. Note that only the F/T sensor mounted at the robot end-effector was used to implement the framework explained in Section III, whereas the OptiTrack and the other F/T sensor were only used for ground truth measurements. The used objects belong to the YCB set [31].

B. Parameters Calibration

To appropriately tune the parameters introduced in Section III, an initial calibration phase was conducted. An expert operator was asked to move the platform in all the three Cartesian directions to properly select the admittance parameters. The smoothing factor α was empirically fixed to 0.01, to attenuate frequency components caused by sensor noise while preserving signal variations associated with human movements. The virtual mass and the virtual damping were set to 2 kg and 2 Ns/m, respectively, for the three axes. Compared to admittance controllers used in related works [15], [22], the damping parameters are notably lower. This choice is due to the fact that, when the platform is moved, the variation of force at the end-effector is low (because of the presence of the cables), hence there is the need of ensuring that also a low variation of force contributes to the movement of the robot. To summarise, mass and damping parameters were selected according to the proposed scenario to ensure accuracy and responsiveness in following human movements.

For the collision distinction algorithm, to have a desired frequency resolution $\Delta\omega \simeq 1$ Hz, given a sampling time $T_s = 0.001$ s, N was selected equal to 1024. The setting time t_{set} for the force calibration phase was chosen equal to 3 s. At this point, the expert user was asked to place and remove different objects from the platform, and to simulate collisions with the environment, along the three directions, both with and without objects placed on the platform. By inspecting the amplitude spectrum, the range of frequencies attributed to contacts was identified, and its lower and upper limits were selected as the boundaries of the frequency interval $[\omega_{\min}, \omega_{\max}]$. In this work, we set $\omega_{\min} = 3$ Hz and $\omega_{\max} = 35$ Hz. Concerning the thresholds for the contact detection, preliminary analysis showed an overlap in the index I_{SND} for rapid changes in collaborative forces and light, minor collisions with the environment. However, following the approach in [23], we opted to establish the thresholds at the maximum values derived from collaborative interactions. This stems from the fact that subtle collisions with the environment, if not immediately detected by the robot, can be easily handled by the human, who can guide the robot back to a safe pose. Accordingly, the index thresholds were established as $I^x_{th} = I^y_{th} = 5$, and $I^z_{th} = 15$ dB/s. The time t_c during which the type of collision is classified is chosen equal to 1 s, while the contact distinction threshold is $F_{th} = 0.15$ N. The time t_r for the object removal detection in absence of detected contact is set to 0.3 s, whereas the tolerance is set as $\epsilon = 0.1$ N.

The parameters for the object placement and removal identification have been empirically selected to guarantee the successful contact distinction in a reasonable range of object weights (approximately from 150 g to 700 g), considering everyday objects [31]. The settings chosen through the calibration procedure described in this section were used for both Exp. A and Exp. B. Note that, in general, while the values of the parameters of the contact detection and distinction determine the method accuracy and should be selected based on task requirements, the admittance parameters affect the robot response to the human steering motions and can be decided also according to users' preferences.

C. Experimental Protocol

Ten participants (6 males and 4 females, age range 25–29) were involved in the experiments. All of them signed an informed consent form (Ethical Approval n. 13/2023, CAREUS Univ. of Siena). Each participant performed a training phase, and then was asked to conduct Exp. A and Exp. B in sequence. In the training phase, users could get acquainted with the system by co-carrying objects with the robot freely, placing different objects on the platform and removing them. In Exp. A, the user was asked to pick a skillet lid (652 g) or the 8 smallest cups (160 g, stuck one inside the other) from an initial location (a table on their left, at a distance of 1.20 m from the robot base), and place them in a final position on their right, 0.54 m far from the robot. In particular, users had to place the lid over a skillet and the cups inside a bigger cup. This process was repeated 10 times, with participants completing 5 trials with one object and 5 trials with the other, alternating between the two. Half of the users started with the lid, while the remaining half with the cups. In Exp. B, users were asked to follow a predefined trajectory, traced with coloured tape on the floor. During this task they had to pick the 8 cups located 1.90 m far from the robot, and place them inside the bigger cup placed at a distance of 1.30 m from the robot. An obstacle was placed 0.80 m far from the robot, in such a way to maximize the possibility of involuntary collisions with it. Participants were instructed to keep their hand position relative to their body fixed, in an ergonomic position. Each user repeated the task 5 times. In both experiments, users started from the same initial position. At the end of the experiments, users were asked to fill in a 5-point Likert scale questionnaire including the statements of the System Usability Scale (SUS) [32], indicated with U1-U10, along with 5 specific statements related to the proposed system, indicated with S1-S5. Possible scores went from "strongly disagree" to "strongly agree". For convenience, we report here all the statements: *U1:* I think that I would like to use this system frequently; *U2:* I found this system unnecessarily complex; *U3:* I thought this system was easy to use; *U4:* I think that I would need assistance to be able to use this system;

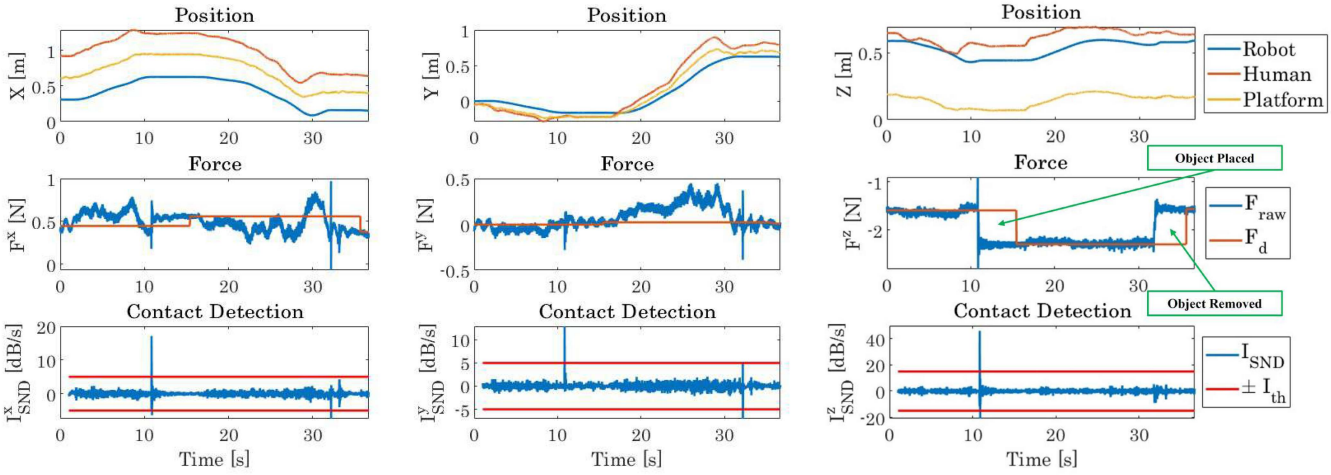

Fig. 5. Representative trial of Exp. A. First row: positions of the robot end-effector, the human hand, and the platform. Second row: force $\mathbf{F}_{raw}$ measured at the end-effector and reference force $\mathbf{F}_d$. Third row: index I_{SND} with the threshold I_{th}. Each column reports values with respect to a different Cartesian axis.

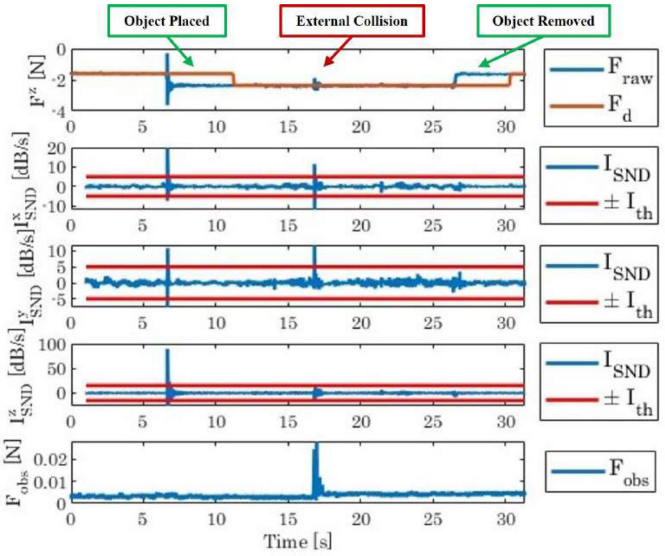

Fig. 6. Representative trial of Exp. B. From top to bottom: *(i)* force $\mathbf{F}_{raw}$ measured at the end-effector and reference force $\mathbf{F}_d$ along the z-axis, *(ii-iv)* index I_{SND} with the threshold I_{th} in the three axes, and *(v)* norm of the force $\mathbf{F}_{obs}$ measured by the F/T sensor fixed on the obstacle.

TABLE I
RESULTS OF THE CONTACT DISTINCTION IN EXP. A.

	Classified as:			
	Placed Objects	**Removed Objects**	**Obstacle Collisions**	**No Contacts**
Placed Objects	99%	0%	0%	1%
Removed Objects	0%	100%	0%	0%

TABLE II
RESULTS OF THE CONTACT DISTINCTION IN EXP. B.

	Classified as:			
	Placed Objects	**Removed Objects**	**Obstacle Collisions**	**No Contacts**
Placed Objects	100%	0%	0%	0%
Removed Objects	0%	100%	0%	0%
External Collisions	0%	0%	84.44%	15.56%

U5: I found the various functions in this system were well integrated; *U6:* I thought there was too much inconsistency in this system; *U7:* I would imagine that most people would learn to use this system very quickly; *U8:* I found this system very cumbersome/awkward to use; *U9:* I felt very confident using this system; *U10:* I needed to learn a lot of things before I could get going with this system; *S1:* I felt safe during the cooperation with the robot; *S2:* I did not trust the robot; *S3:* The robot was following me easily; *S4:* The robot did not understand my intentions; *S5:* Following a pre-defined trajectory was difficult.

D. Results and Discussion

The working principles of our method can be observed in Figs. 5 and 6, where representative trials of Exp. A and Exp. B are reported, respectively. The system objective performance in terms of percentage of correct contact distinctions is summarized in Table I and Table II, whereas the users' subjective feedback is shown in Fig. 7.

Let us consider Fig. 5. By looking at the graphs at the top, reporting the x, y, and z trajectories of the human hand, the robot end-effector, and the platform, it can be noticed that the robot accurately follows the human motion. When the human moves, the measured force at the end-effector deviates from the desired force (see graphs in the middle layer) and this prompts the robot to adjust to regain the desired configuration of the platform, and reduce the force error to zero. The placement of the object ($t \approx 11$ s) is identified by the collision algorithm across all the three axes (see the contact distinction index in the bottom layer), leading to the recalibration of the desired force in the

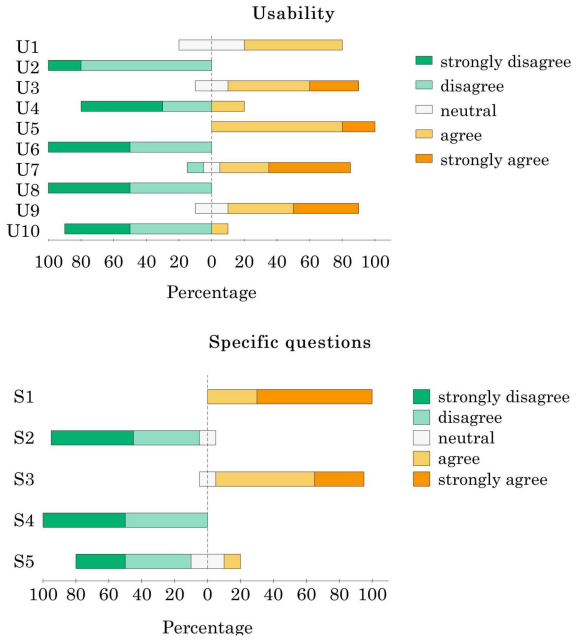

Fig. 7. Replies to the subjective questionnaires.

following seconds (see F^z). The removal of the object ($t \approx 32$ s) is recognized on the x and y axes (I^x_{SND} and I^y_{SND} exceed the threshold), while not on the z -axis, and the desired force is recalibrated accordingly. As reported in Table I, only 3 failures occured out of 100 trials: 1 for an unrecognized object placed, and 2 in the transport of the object. The former occured with the cups, and the latters occured with the lid which slipped on the platform. Additionally, over all trials, only 3 contacts were detected despite no actual contact occurred (false positives).

Let us now consider Exp. B. As shown in Fig. 6, both the placement of the object on the platform ($t \approx 7$ s) and the external collision with the obstacle ($t \approx 17$ s) trigger a contact detection (see graphs reporting I_{SND} in the three components). The contact distinction classifies the detected contacts accurately as shown by the fact that the desired force is recalibrated only after the object placement (see the graph related to F^z at $t \approx 11$ s). Notably, at the end of the trial, the object removal does not trigger any contact detection, yet it is correctly identified by the proposed method, as shown by the change in F^z_{des} at $t \approx 30$. As summarized in Table II, all placements and removals of the object were correctly detected. Concerning the collisions with external obstacles, 45 collisions with the box actually occurred during the experiments and only the 15.56% of these were not detected by the algorithm. Failures occurred mainly in correspondence of collisions having a lighter intensity. Anyway, no failures in the object transportation occurred in Exp. B. Additionally, over all trials, only 4 contacts were detected despite no actual contact occurred.

The removal of the object was always correctly detected both in Exp. A and Exp. B. This was due to the dual way of tackling the removal detection explained in Section III-B. In the 27.33% of the 150 trials, object removals did not trigger any contact detection, yet they were correctly identified through the alternative method based on thresholds on the z component of the measured force. This shows the effectiveness of the proposed methodology.

The average norm of the translational velocity of the robot end-effector, across all trials and users, was $\simeq 0.050$ m/s in Exp. A and $\simeq 0.049$ m/s in Exp. B. The average task completion time was 36.37 s for Exp. A, and 44.46 s for Exp. B. Higher or lower values of velocity may be obtained changing adequately the control parameters, and this, in turn, would influence the completion time. The average norm of the force $\mathbf{F}_a$, corresponding to the force arising from the users' movements, was 0.23 N in Exp. A, and 0.22 N in Exp. B. These values demonstrate the low force required by the users to push or pull the robot to move the platform in the desired pose, thanks to the suitably selected admittance parameters and the introduction of cables in the system.

According to participants' responses (Fig. 7) the system obtained an average SUS score of 79.5, well above the average SUS score for a usable system, which is considered to be 68 [33]. Regarding the specific questions, all users agreed with S1 and $9/10$ of them disagreed with S2. This means that overall they felt rather safe and confident during the collaboration. Users also evaluated positively the capability of the robot of following the human during the collaborative transportation (S3, S4), and most of them ($7/10$) did not have problems in following a predefined trajectory while co-carrying items with the robot in Exp. B (S5).

V. Conclusion

This work introduces the novel scenario of collaborative human-robot cable-suspended manipulation. The use of cables allows to extend the workspace of the collaboration, while at the same time ensuring operator safety and introducing an intrinsic compliance in the system guaranteeing lower exchanged forces. A strategy based on admittance control was implemented to allow the robot to follow the user and maintain the platform in equilibrium to accomplish the task. In addition, a contact detection and distinction method was developed to distinguish the voluntary steering motions of the human from placements or removals of objects and from external collisions with obstacles. Two validation experiments involving 10 participants demonstrated the system usability and reliability in detecting and distinguishing contacts.

The proposed method is particularly suitable for unstructured environments as it relies only on force measurements at the robot end-effector and does not need any a priori knowledge on the physical properties of the platform and the objects. These are implicitly taken into account in the calibration phase to set the thresholds required in the contact detection and distinction routines. Despite requiring an initial tuning of the parameters, the proposed threshold-based approach for contact handling ensures fast robot reactions. Future work will focus on devising algorithms for the on-line adaptation of thresholds, e.g., based on the object weight. Additionally, we will investigate novel approaches, possibly data-driven, to optimise the selection of time intervals, thresholds, and admittance parameters for more complex and faster transportation scenarios, with a wider range of objects.

In the current setting, the human operator leads the collaborative task, but their control over the robot is suspended for a short time when a contact is detected and when the robot needs to recover from an unintended collision. In these events, the human understands the robot behaviour by direct visual feedback, but is not fully aware of whether the robot correctly understood the type of contact, or of when the robot will actually resume the collaboration. Providing the user with this information can be very important to achieve a more fluent interaction. In the upcoming developments of the work, we will investigate the use of wearable tactile interfaces for improved human awareness. A limitation of the current approach is that uncontrollable oscillations of the platform, as well as the possible object slippage, are not explicitly handled with reactive robot actions, thus it is the human who has to manage them. Despite in the conducted experiments these phenomena did not significantly affect the task success rate, future work will address them, conducting a more detailed investigation to characterize the dynamics and stability of the system.

This work paves the way for future advancements in human-robot collaborative manipulation, offering new possibilities for enhancing efficiency and safety in shared workspaces, both in industrial and assistive applications.

REFERENCES

[1] V. Villani, F. Pini, F. Leali, and C. Secchi, "Survey on human–robot collaboration in industrial settings: Safety, intuitive interfaces and applications," *Mechatronics*, vol. 55, pp. 248–266, 2018.

[2] D. Prattichizzo et al., "Human augmentation by wearable supernumerary robotic limbs: Review and perspectives," *Prog. Biomed. Eng.*, vol. 3, no. 4, 2021, Art. no. 042005.

[3] C. A. Parker and E. A. Croft, "Design & personalization of a cooperative carrying robot controller," in *Proc. 2012 IEEE Int. Conf. Robot. Automat.*, 2012, pp. 3916–3921.

[4] A. Bussy, P. Gergondet, A. Kheddar, F. Keith, and A. Crosnier, "Proactive behavior of a humanoid robot in a haptic transportation task with a human partner," in *Proc. IEEE RO-MAN, 21st IEEE Int. Symp. Robot Hum. Interactive Commun.*, 2012, pp. 962–967.

[5] A. Mörtl, M. Lawitzky, A. Kucukyilmaz, M. Sezgin, C. Basdogan, and S. Hirche, "The role of roles: Physical cooperation between humans and robots," *Int. J. Robot. Res.*, vol. 31, no. 13, pp. 1656–1674, 2012.

[6] J. E. Solanes, L. Gracia, P. Munoz-Benavent, J. V. Miro, M. G. Carmichael, and J. Tornero, "Human–robot collaboration for safe object transportation using force feedback," *Robot. Auton. Syst.*, vol. 107, pp. 196–208, 2018.

[7] S. Marullo, M. Pozzi, D. Prattichizzo, and M. Malvezzi, "Cooperative human-robot grasping with extended contact patches," *IEEE Robot. Automat. Lett.*, vol. 5, no. 2, pp. 3121–3128, Apr. 2020.

[8] M. L. Elwin, B. Strong, R. A. Freeman, and K. M. Lynch, "Human-multirobot collaborative mobile manipulation: The omnid mocobots," *IEEE Robot. Automat. Lett.*, vol. 8, no. 1, pp. 376–383, Jan. 2023.

[9] M. Mujica, M. Crespo, M. Benoussaad, S. Junco, and J.-Y. Fourquet, "Robust variable admittance control for human–robot co-manipulation of objects with unknown load," *Robot. Comput.- Integr. Manuf.*, vol. 79, 2023, Art. no. 102408.

[10] D. M. Nguyen et al., "Human uncertainty-aware MPC for enhanced human-robot collaborative manipulation," in *Proc. IEEE 7th Int. Conf. Ind. Cyber-Phys. Syst.*, 2024, pp. 1–6.

[11] P. Franceschi, D. Cassinelli, N. Pedrocchi, M. Beschi, and P. Rocco, "Design of an assistive controller for physical human–robot interaction based on cooperative game theory and human intention estimation," *IEEE Trans. Automat. Sci. Eng.*, early access, Jul. 22, 2024, doi: 10.1109/TASE.2024.3429643.

[12] D. Kruse, R. J. Radke, and J. T. Wen, "Collaborative human-robot manipulation of highly deformable materials," in *Proc. 2015 IEEE Int. Conf. Robot. Automat.*, 2015, pp. 3782–3787.

[13] J. DelPreto and D. Rus, "Sharing the load: Human-robot team lifting using muscle activity," in *Proc. IEEE 2019 Int. Conf. Robot. Automat.*, 2019, pp. 7906–7912.

[14] D. Sirintuna, A. Giammarino, and A. Ajoudani, "An object deformation-agnostic framework for human–robot collaborative transportation," *IEEE Trans. Automat. Sci. Eng.*, vol. 21, no. 2, pp. 1986–1999, Apr. 2024.

[15] D. Sirintuna, I. Ozdamar, and A. Ajoudani, "Carrying the uncarriable: A deformation-agnostic and human-cooperative framework for unwieldy objects using multiple robots," in *Proc. 2023 IEEE Int. Conf. Robot. Automat.*, 2023, pp. 7497–7503.

[16] A. Alp and S. Agrawal, "Cable suspended robots: Design, planning and control," in *Proc. 2002 IEEE Int. Conf. Robot. Automat. (Cat. No.02CH37292)*, 2002, pp. 4275–4280.

[17] M. Carricato et al., "Static workspace computation for underactuated cable-driven parallel robots," *Mechanism Mach. Theory*, vol. 193, 2024, Art. no. 105551.

[18] P. Prajapati, S. Parekh, and V. Vashista, "Collaborative transportation of cable-suspended payload using two quadcopters with human in the loop," in *Proc. 2019 28th IEEE Int. Conf. Robot Hum. Interactive Commun.*, 2019, pp. 1–6.

[19] D. Sanalitro, H. J. Savino, M. Tognon, J. Cortés, and A. Franchi, "Full-pose manipulation control of a cable-suspended load with multiple UAVs under uncertainties," *IEEE Robot. Automat. Lett.*, vol. 5, no. 2, pp. 2185–2191, Apr. 2020.

[20] B. E. Jackson, T. A. Howell, K. Shah, M. Schwager, and Z. Manchester, "Scalable cooperative transport of cable-suspended loads with UAVs using distributed trajectory optimization," *IEEE Robot. Automat. Lett.*, vol. 5, no. 2, pp. 3368–3374, Apr. 2020.

[21] G. Li, X. Liu, and G. Loianno, "Human-aware physical human-robot collaborative transportation and manipulation with multiple aerial robots," *IEEE Trans. Robot.*, 2024.

[22] V. Duchaine and C. Gosselin, "Safe, stable and intuitive control for physical human-robot interaction," in *Proc. 2009 IEEE Int. Conf. Robot. Automat.*, 2009, pp. 3383–3388.

[23] A. Kouris, F. Dimeas, and N. Aspragathos, "A frequency domain approach for contact type distinction in human–robot collaboration," *IEEE Robot. Automat. Lett.*, vol. 3, no. 2, pp. 720–727, Apr. 2018.

[24] F. Caccavale and M. Uchiyama, "Cooperative manipulation," in *Springer Handbook of Robotics*. Berlin, Germany: Springer, 2016, pp. 989–1006.

[25] S. Haddadin, A. De Luca, and A. Albu-Schäffer, "Robot collisions: A survey on detection, isolation, and identification," *IEEE Trans. Robot.*, vol. 33, no. 6, pp. 1292–1312, Dec. 2017.

[26] S. Golz, C. Osendorfer, and S. Haddadin, "Using tactile sensation for learning contact knowledge: Discriminate collision from physical interaction," in *Proc. 2015 IEEE Int. Conf. Robot. Automat.*, 2015, pp. 3788–3794.

[27] F. Franzel, T. Eiband, and D. Lee, "Detection of collaboration and collision events during contact task execution," in *Proc. 2020 IEEE-RAS 20th Int. Conf. Humanoid Robots (Humanoids)*, 2021, pp. 376–383.

[28] M. Lippi and A. Marino, "Enabling physical human-robot collaboration through contact classification and reaction," in *Proc. 2020 29th IEEE Int. Conf. Robot Hum. Interactive Commun.*, 2020, pp. 1196–1203.

[29] A. Kouris, F. Dimeas, and N. Aspragathos, "Contact distinction in human-robot cooperation with admittance control," in *Proc. 2016 IEEE Int. Conf. Syst., Man, Cybern.*, 2016, pp. 001951–001956.

[30] A. Thakker, "Seamless integration of optitrack motion capture with ros," Version v1, vol. 1, 2022.

[31] B. Calli, A. Walsman, A. Singh, S. Srinivasa, P. Abbeel, and A. M. Dollar, "Benchmarking in manipulation research: Using the Yale-CMU-Berkeley object and model set," *IEEE Robot. Automat. Mag.*, vol. 22, no. 3, pp. 36–52, Sep. 2015.

[32] J. Brooke et al., "SUS: A quick and dirty usability scale," *Usability Eval. Ind.*, vol. 189, no. 194, pp. 4–7, 1996.

[33] J. Sauro, "A practical guide to the system usability scale: Background, benchmarks & best practices," *Measuring Usability LLC*, 2011.

Open Access funding provided by 'Università degli Studi di Siena' within the CRUI CARE Agreement